

PAPER • OPEN ACCESS

Investigation of resistance and intermetallic layer formation in laser-welded joints between Copper and AM Aluminium for electrical connections

To cite this article: Aki Piironen *et al* 2025 *IOP Conf. Ser.: Mater. Sci. Eng.* **1332** 012026

View the [article online](#) for updates and enhancements.

You may also like

- [Study on Welding Process of 7x0.5 Multilayer 304 Bellows and Flange](#)
Zhaodong Jiang, Dong Liang, Tong Zhou et al.
- [Research on automatic welding system for oil and gas pipeline based on laser tracking technology](#)
Shaozhu Liu, Zhiqiang Bi, Congcong Xu et al.
- [Three axis milling machine applications for welding samples test neutron instrument using friction stir welding method](#)
Muhamad Saparudin, Tri Hardi Priyanto, Rifky Apriansyah et al.



The Electrochemical Society
Advancing solid state & electrochemical science & technology



249th
ECS Meeting
May 24-28, 2026
Seattle, WA, US
Washington State
Convention Center

Spotlight Your Science

**Submission deadline:
December 5, 2025**

SUBMIT YOUR ABSTRACT

Investigation of resistance and intermetallic layer formation in laser-welded joints between Copper and AM Aluminium for electrical connections

Aki Piironen^{1*}, Antti Salminen¹, Joonas Pekkarinen²

¹University of Turku, Department of Mechanical and Materials Engineering, Finland,

²Turku University of Applied Sciences, Dept. Mechanical Engineering

*E-mail: aki.piironen@utu.fi

Abstract. The increasing electrification of transportation demands the development of more energy-efficient solutions, where additive manufacturing (AM) of electrically conductive components presents new opportunities. The design flexibility of AM enables unique innovations; however, it also introduces challenges due to additional process parameters affecting part production. A key concern in the use of laser powder bed fusion of metal (PBF-LB/M) manufactured parts is their material properties, which are further influenced by part plane orientation during fabrication. Previous research has focused on copper-aluminum dissimilar welding, but the specific challenges posed by AM techniques have not been fully explored. This study investigates the welding behavior concerning resistance and intermetallic layer formation. Nickel-plated copper sheet metal samples were welded to AM aluminium samples using a continuous wave single-mode fiber laser with scanner optics in a lap joint configuration. Before welding, the interface surface of the AM samples was machined to exclude the surface roughness variance effect on the result. During the experiments, the welding's optical laser power was constant at 2kW and variations were made in welding speed ranging from 1200 mm/s to 400 mm/s in 200 mm/s increments. Electrical resistance measurements were taken using a high-precision micro resistance meter with a 4-wire Kelvin testing method, also hardness testing, tensile testing, and energy dispersive spectroscopy (EDS) analysis were conducted. The results revealed that intermetallic compounds formed during welding, influencing joint properties. At a lower welding speed, more aluminium was mixed with copper which led to the weld solidification cracking. The optimum welding speed was between 800 and 1000 mm/s for this study test setup.



1. Introduction

The ongoing electrification of transportation is driving the demand for more energy-efficient and compact solutions, particularly in the field of high-power electrical components. Additive manufacturing (AM) offers a promising avenue for producing electrically conductive components with complex geometries, weight reduction, integrated cooling, and enhanced design flexibility. However, while AM opens up new design possibilities, it also introduces significant challenges, especially in terms of process reliability, microstructural control, and electrical performance.

Among AM materials, AlSi10Mg produced by laser powder bed fusion (PBF-LB/M) has emerged as a strong candidate for electrical applications due to its favorable combination of mechanical strength and electrical conductivity. However, its electrical conductivity is not a fixed property. Research indicates that the resistivity of AlSi10Mg varies with build orientation and post-processing. Vertically built samples show lower resistivity (average $7.78 \mu\Omega\cdot\text{cm}$) than horizontally built ones (average $9.87 \mu\Omega\cdot\text{cm}$), while post-heat treatments reduce resistivity by up to 33% and eliminate anisotropy caused by build orientation. A major limitation in using AM components for electrical applications is the integrity of welded joints. These joints are critical for reliable system integration. One recurring issue is the significantly higher pore susceptibility in laser-welded PBF-LB/M aluminium compared to conventionally manufactured alloys. [1,2,3]

In high-performance electrical systems such as battery cells, aluminium (Al) and copper (Cu) are widely used due to their excellent conductivity, corrosion resistance, and low weight. However, laser welding of dissimilar Al–Cu joints is challenging. The significant differences in their physical and thermal properties, such as melting point, thermal conductivity, and thermal expansion, lead to welding difficulties. Moreover, the limited solubility of copper in aluminum promotes the formation of brittle intermetallic compounds (IMCs), which degrade both the mechanical and electrical performance of the joint. A thicker IMC layer further contributes to increased brittleness and contact resistance. Controlling process parameters, like welding speed, is essential to balance metallurgical bonding while limiting the formation of brittle phases. To improve the joining performance of Al and Cu, research indicates that a smaller laser spot diameter with lower overall power minimizes the formation of intermetallic compounds by providing better control of penetration depth and mixing of base materials. Brittle fracture behavior was recorded with the large spot size, while ductile behavior was recorded with the smaller one. It also demonstrates that increasing the laser welding speed reduces the amount of intermetallic compounds formed and improves the tensile properties of the joint. Previous research also shows that the electrical conductivity of a weld cannot necessarily be increased by increasing the surface area of the weld; in fact, it may even weaken the conductivity of the joint. Weld placements play a more significant role in resistance than increasing the surface area of the joint. [4,5,6,7,8,9,10]

While prior studies have explored Al–Cu dissimilar welding, the resistivity of AM AlSi10Mg, and the laser welding behavior of AlSi10Mg separately, this study presents a novel approach by integrating all these aspects. The objective is to assess the weldability and intermetallic formation of AM-fabricated AlSi10Mg components when joined with nickel-plated copper.

2. Experimental setup

This study uses nickel-plated 0.2 mm thick pure copper (Cu) (9,30 x 40 mm) sheets and powder bed fusion (PBF-LB/M) manufactured AlSi10Mg aluminum alloy test samples (Figure 1). These AM samples were arranged in a nested configuration with seven distinct build angles. The build angles were from -30 to 30 degrees with 10-degree intervals. Test pieces were manufactured using an SLM Solutions 280 2.0 TWIN 700W AM machine. According to powder material provider SLM Solutions, the powder particle size of the AlSi10Mg material is 20 – 63 μm and in spherical shape. The density of the material is $\geq 99.0 - 99.5\%$.

For post-processing AM samples were glass bead blasted. To mitigate the influence of surface roughness variability on the welding process, 0.2 mm was machined from the weld interface surface.

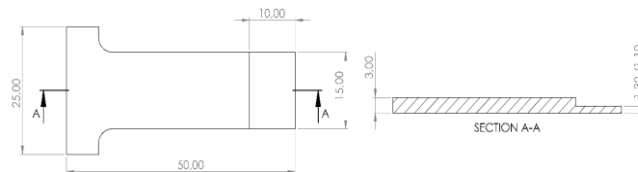


Figure 1. Powder bed fusion (PBF-LB/M) manufactured AlSi10Mg aluminum alloy test sample drawing.

Before welding, the electrical resistance of each AM aluminium sample was measured using a four-wire Kelvin testing method with a Hioki RM3534 high-precision resistance meter, which provides a resolution of 0.01 $\mu\Omega$. A custom measurement fixture was employed to ensure consistent contact and maintain a constant 29 mm spacing between the measurement clip probes as shown in figure 2a. Each sample was measured five times, and the average value was calculated to assess the impact of build orientation on resistance.

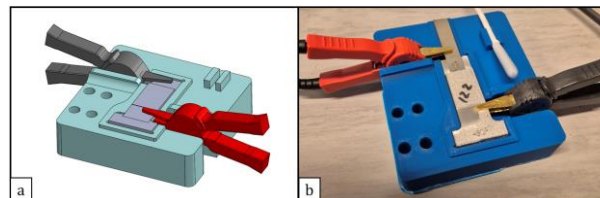


Figure 2. Resistance measuring fixture, a) AM sample testing, b) Measurement of welded sample

Subsequently, copper-aluminium lap joint welds were produced, with the copper sheet placed on top of the AM aluminium test samples. Welding was performed using a continuous-wave IPG YLS-2000SM single-mode fiber laser equipped with Arges Elephant 3D scanner optics. The Arges Elephant is a 3D galvanometer scanner featuring a 50 mm aperture and a 60 μm focal spot diameter. The laser beam was focused on the top surface of the copper sheet, and no shielding gas was used during the welding process. The laser power was kept constant at 2000 W across all experiments. Welding speeds ranged from 1200 mm/s to 400 mm/s in 200 mm/s increments. All welds followed a circular path with a diameter of 3 mm. Total welding times varied from 23ms to 48ms including scanner mirror movements before welding.

In total, 35 welded samples were fabricated, with 7 samples prepared for each of the five welding speeds. Each of the seven samples corresponded to a distinct AM build orientation. The electrical resistance of the welded joints was measured using the same four-wire method and a similar measurement fixture used for the base material, maintaining the 40 mm clip probe spacing as shown in figure 2b.

Metallographic cross-sections were prepared from each welding speed test set to examine the weld interface. Sample selection was based on AM aluminium manufacturing angle so that all selected samples were manufactured in a vertical position. These cross-sections were imaged using an optical microscope and a Thermo Scientific Apreo S field-emission scanning electron microscope (FE-SEM), coupled with an Oxford Instruments UltimMax 100 energy-dispersive X-ray spectroscopy (EDS) detector for elemental analysis. Vertical microhardness profiles with 0.1 mm step movement were obtained (HV0.3) from the cross-sections using a Falcon 600 microhardness tester to evaluate hardness variations across the weld.

The remaining samples were subjected to tensile testing using a Testometric M350-10CT universal testing machine to assess the mechanical performance of the welds. The combined results from resistance measurements, SEM/EDS analysis, microhardness testing, and tensile testing were used to evaluate the influence of welding parameters and build orientation on the quality of the copper–aluminium joints.

3. Results and discussion

3.1 Resistance measurements

Preliminary four-wire micro-resistance measurements conducted on the machined and post-processed AM test specimens indicated that the build orientation had no significant effect on the electrical resistance of the samples. This may be due to the manufacturing angle variance being only 30 degrees off vertical and the accuracy of the measurement method was not necessarily sufficient to detect differences. A total of seven sets of specimens were measured, each representing all of the seven different build orientations. The average resistance values across all separate build orientations ranged from 47.1 to 48.1 $\mu\Omega$ with an overall average resistance value of 47.4 $\mu\Omega$ (R_{AL}) (standard deviation of 2,2 $\mu\Omega$) with a 29 mm clip probe measurement distance. The lowest recorded individual resistance value was 39.3 $\mu\Omega$, while the highest was 57.9 $\mu\Omega$. Correspondingly, the resistance of the nickel-plated 0.2 mm thick copper sheet was measured at 95.6 $\mu\Omega$ (R_{CU}) (standard deviation of 4,3 $\mu\Omega$) with a 10 mm clip probe measurement distance. If we calculate material resistivity based on these measurement values, we get a resistivity value for 6.54 $\mu\Omega \cdot \text{cm}$ aluminium and 1.81 $\mu\Omega \cdot \text{cm}$ for copper. AM aluminium value being higher than pure aluminium 2.65 $\mu\Omega \cdot \text{cm}$ (at 20°C) but very close to the AlSi10Mg powder data sheet value 6.90 $\mu\Omega \cdot \text{cm}$. Nickel plated copper sample resistivity value is very close of the resistivity of pure copper 1.68 $\mu\Omega \cdot \text{cm}$ (at 20°C).

Micro-resistance measurements over weld joints with different welding speeds resulted resistance average values ranging from 174.2 to 182.5 $\mu\Omega$ with an overall average resistance value 177.5 $\mu\Omega$ (standard deviation of 19,9 $\mu\Omega$). The highest resistance values were measured with welding speed 1200 mm/s 182,5 $\mu\Omega$ and 400 mm/s 181,9 $\mu\Omega$. With welding speeds 1000mm/s, 800 mm/s and 600 mm/s the average resistance value per welding speed was 174 $\mu\Omega$. Figure 3 shows a schematic of welded sample serial resistance components. If we calculate weld interface resistance R_{AlCu} using average values of R_{CU} (95.6 $\mu\Omega$), R_{AL} (47.4 $\mu\Omega$), and average values of all weld measurements 177.5 $\mu\Omega$ we get the resistance value for weld interface 34.5 $\mu\Omega$. While there is no fixed standard exists to compare the measurement results values to industry applications. High-current applications such as EV busbars typically target joint resistances below 100 $\mu\Omega$ and many designs strive for values significantly lower. A 10 $\mu\Omega$ increase at 100 A produces 0.1 W per joint, leading to significant cumulative thermal load in multi-joint systems.

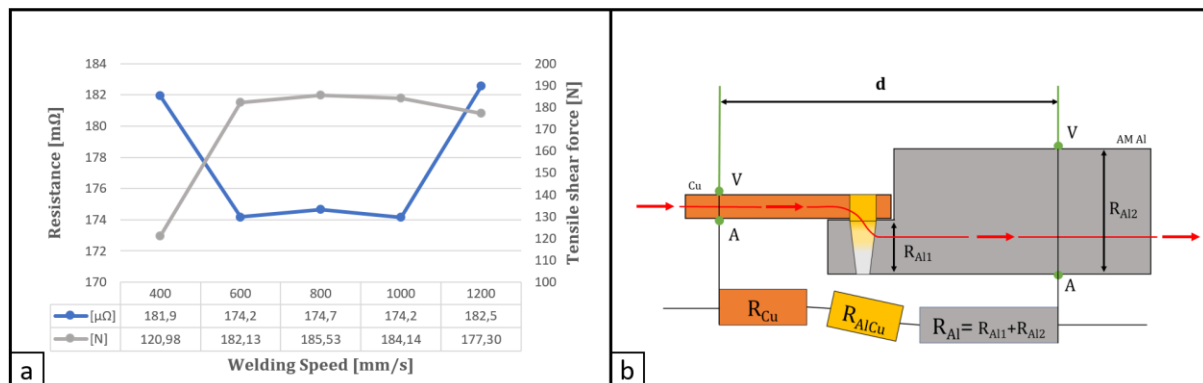


Figure 3. a) Test welds resistance and tensile shear force results. b) Serial resistance of on an overlap welded sample

3.2 Microhardness testing

Microhardness testing (HV0.3) revealed that the base material hardness of copper was in Vickers hardness 74 HV, while the average hardness of the AM aluminium was 120 HV. A vertical hardness profile measured along the weld centerline indicated the intermixing of the two metals at all welding speeds, forming high-hardness intermetallic compound (IMC) phases. The hardness values of these IMC phases in the upper region of the weld varied between 192 and 687 HV. The hardness profiles shown in Figure 4 are nearly identical across all welding speeds, with the exception of the 1200 mm/s case, where aluminium exhibited less intermixing with copper. The hardness values in the lower weld region, even at slower welding speeds with deeper penetration, match those of the base aluminum, indicating a lack of material mixing

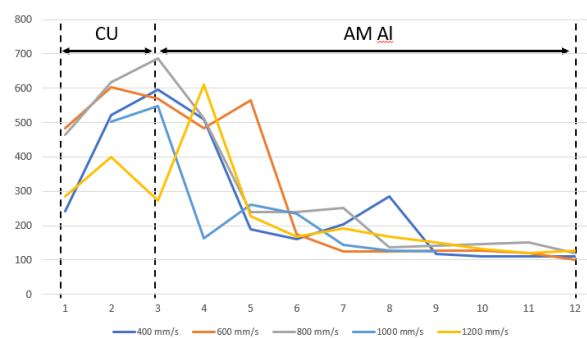


Figure 4. A vertical microhardness (HV0.3) profiles with different welding speeds measured along the weld centreline.

3.3 Tensile testing

The average tensile strengths at different welding speeds followed a similar trend to that observed in the resistance measurements. The lowest tensile strengths were recorded at the highest (1200 mm/s) and lowest (400 mm/s) welding speeds, with values of 177 N and 121 N, respectively. In contrast, intermediate welding speeds of 1000 mm/s, 800 mm/s, and 600 mm/s resulted in slightly higher and more consistent ductile tensile strengths: 184 N, 186 N, and 182 N.

Notably, at 1200 mm/s, the limited fusion and shallow penetration, as seen in the cross-sectional images (Attachment 1), resulted in weak metallurgical bonding. This structural weakness was reflected in tensile testing, where two out of six samples failed below 20 N, and all fractures occurred within the weld itself rather than in the base material signaling poor weld integrity.

3.4 Microstructural and Elemental Analysis of Weld Cross-Sections

Cross-sectional analysis of Cu-AM Al lap welds produced at five welding speeds (1200–400 mm/s). At 1200 mm/s, the fusion zone is narrow. The elemental maps show a clear boundary between the two materials, and only minor diffusion of elements across the interface is observed with minimal intermixing and limited intermetallic compound (IMC) formation. As speed decreases to 1000 mm/s, a deeper fusion zone and increased Cu-Al diffusion are observed. At 800 mm/s, the weld interface shows more uniform mixing, with SEM-EDS confirming strong elemental diffusion. Welding at 600 mm/s results in a larger fusion zone with deeper penetration and more pronounced IMC formation, particularly at the top weld section. At 400 mm/s, excessive heat input leads to deep penetration, extensive Cu-Al mixing, and widespread IMC formation.

Cracks were observed at 600 and 400 mm/s, initiating at the weld top where temperature gradients and IMC growth are highest. These regions also correspond to elevated hardness values, indicating brittle microstructures. The results demonstrate that welding speeds below 600 mm/s compromise joint integrity due to increased IMC-induced brittleness and crack formation. Thus, lower speeds are not recommended for reliable Cu-AM Al joints.

4. Conclusion

This study examined lap joint welds between nickel-plated copper and AlSi10Mg aluminum alloy samples produced by laser powder bed fusion (PBF-LB/M) using high-speed laser welding. It focused on how different welding speeds affect the mechanical, microstructural, and electrical properties of the welds. AM AlSi10Mg samples' initial electrical resistance measurements showed no significant variation from the additive manufacturing build orientation. However, post-weld resistance increased at both low and high welding speeds, correlating with mechanical and microstructural changes. Hardness testing revealed hard intermetallic compounds (IMCs) forming within the welds, with peak hardness reaching 687 HV at 800 mm/s. Imaging techniques showed cracks and brittleness due to excessive intermixing at slower speeds. Tensile strength was highest and most consistent at intermediate welding speeds (800–1000 mm/s), reaching 182–186 N. Speeds outside this range resulted in weaker welds due to poor penetration or brittleness.

The study concluded that the optimal welding speed with a 2kW laser power range for balancing mechanical strength, controlled IMC formation, and electrical performance lies between 800 and 1000 mm/s. Future work is suggested to include more localized microscale resistance mapping for each IMC phase to understand the weld interface better.

References

- [1] Silbernagel C, Ashcroft I, Dickens P, Galea M. 2018 . *Addit Manuf.* May **21**:395–403.
- [2] Mäkikangas J, Rautio T, Mustakangas A, Mäntyjärvi K. 2019 *Procedia Manuf.* **36**:88–94.
- [3] Nunes R, Faes K, De Waele W, Simar A, Verlinde W, Lezaack M, et al. 2023 *Metals.* Oct 10;**13**(10):1724.
- [4] Sadeghian A, Iqbal N. 2022. *Opt Laser Technol.* Feb;**146**:107595.
- [5] Hollatz S, Kremer S, Ünlübayir C, Sauer DU, Olowinsky A, Gillner 2020 *Batteries.* Apr 21;**6**(2):24.
- [6] Kah P, Vimalraj C, Martikainen J, Suoranta R. 2015 *Int J Mech Mater Eng.* Dec;**10**(1):10.
- [7] Dimatteo V, Ascari A, Liverani E, Fortunato 2022 *Opt Laser Technol.* Jan;**145**:107495.
- [8] Lee K, Rinker TJ, Pour MM, Cai W, Huang W, Tan W, et al. 2023. *Manuf Lett.* Aug;**35**:221–31.
- [9] Ali S, Shin J. 2022 *Materials.* Oct 25;**15**(21):7463.
- [10] Zuo D, Hu S, Shen J, Xue Z. 2014. *Mater Des.* Jun;**58**:357–62.